

NASA TECHNICAL  
MEMORANDUM

NASA TM X-53722

April 10, 1968

NASA TM X-53722

GPO PRICE \$ \_\_\_\_\_

CFSTI PRICE(S) \$ \_\_\_\_\_

Hard copy (HC) 300

Microfiche (MF) 65

ff 653 July 65

DAMPING OF THERMOELASTIC STRUCTURES

By William Mitchell Gillis  
Aero-Astrodynamic Laboratory

FACILITY FORM 602

N 68-27903  
(ACCESSION NUMBER)

(THRU)

57  
(PAGES)

(CODE)

TMX-53722  
(NASA CR OR TMX OR AD NUMBER)

32  
(CATEGORY)

NASA

*George C. Marshall  
Space Flight Center,  
Huntsville, Alabama*

TECHNICAL MEMORANDUM X-53722

DAMPING OF THERMOELASTIC STRUCTURES

By

William Mitchell Gillis

George C. Marshall Space Flight Center

Huntsville, Alabama

ABSTRACT

This report considers longitudinal waves traveling in a cylindrical rod. After a review of the classical results of wave propagation in unbounded elastic solids and in elastic cylinders, the subject of thermal modification of elastic properties is undertaken. The resultant effects upon the purely elastic wave motion consists of a change in the propagation velocity and the addition of a damping effect upon the mechanical energy of the elastic wave due to heat conduction. The thermoelastic effects upon a longitudinal elastic wave are shown to be small in terms of the propagation velocity. However, more significantly, the thermoelastic damping effect is large for very high frequency waves traveling in small diameter bars. The behavior of the thermoelastic damping coefficient is linked to a "thermoelastic bar number," developed herein. Finally, approximations are developed, based upon the value of the thermoelastic bar number, to predict the behavior of the thermoelastic damping coefficient as a function of frequency.

NASA - GEORGE C. MARSHALL SPACE FLIGHT CENTER

---

Technical Memorandum X-53722

---

April 10, 1968

DAMPING OF THERMOELASTIC STRUCTURES

By

William Mitchell Gillis

ORBITAL MECHANICS SECTION  
MISSION ANALYSIS BRANCH  
DYNAMICS AND FLIGHT MECHANICS DIVISION  
AERO-ASTRODYNAMICS LABORATORY  
RESEARCH AND DEVELOPMENT OPERATIONS

## TABLE OF CONTENTS

	<u>Page</u>
INTRODUCTION.....	1
CHAPTER I.    WAVE PROPAGATION IN AN INFINITE ELASTIC SOLID	
A.    The Equations of Motion.....	3
B.    Wave Propagation.....	9
CHAPTER II.    LONGITUDINAL ELASTIC WAVE PROPAGATION IN CYLINDRICAL RODS	
A.    Elementary Theory.....	11
B.    Rayleigh-Love Correction.....	14
C.    Mindlin and Herrmann's Method.....	17
D.    Bishop's Method.....	19
E.    Comparison of Bishop's Method and Herrmann and Mindlin's Method.....	24
F.    Improved Longitudinal Wave Equation.....	26
CHAPTER III.    THERMOELASTIC WAVES	
A.    Thermoelastic Equations of Motion.....	29
B.    Uncoupled Solution.....	33
C.    Coupled Solution.....	34
D.    Numerical Results.....	36
E.    Limiting Case for $a/L$ Approach Zero.....	42
F.    Thermoelastic Bar Number.....	44
CONCLUSIONS.....	47
BIBLIOGRAPHY.....	48

## LIST OF ILLUSTRATIONS

<u>Figure</u>	<u>Title</u>	<u>Page</u>
1	Coordinate System Definition.....	4
2	Longitudinal Elastic Wave Propagation Velocity as a Function of Radius to Wavelength Ratio....	25
3	Longitudinal Thermoelastic Wave Propagation Velocity as a Function of Reduced Frequency....	37
4	Longitudinal Thermoelastic Wave Velocity as a Function of Radius to Wavelength Ratio.....	39
5	Thermoelastic Damping Coefficient as a Function of Reduced Frequency.....	40
6	Thermoelastic Damping Coefficient as a Function of Radius to Wavelength Ratio.....	41
7	Effect of Thermoelastic Bar Number ( $d\nu X$ ).....	46

## LIST OF SYMBOLS

<u>Symbol</u>	<u>Definition</u>
$r, \theta, z$	cylindrical coordinates
$U, V, W$	displacements along the coordinate axes
$\rho$	mass per unit volume
$\sigma_r, \sigma_\theta, \sigma_z$	normal stresses in the direction of the coordinate axes
$\tau_{r\theta}, \tau_{rz}, \tau_{\theta z}$	shear stresses
$\epsilon_r, \epsilon_\theta, \epsilon_z$	normal strains in the direction of the coordinate axes
$\Delta$	dilatation
$\gamma_{r\theta}, \gamma_{rz}, \gamma_{\theta z}$	shear strains
$\bar{\omega}_r, \bar{\omega}_\theta, \bar{\omega}_z$	rotation about the coordinate axes
$E$	Young's modulus
$\nu$	Poisson's ratio
$\lambda, \mu$	Lame's constants
$\nabla$	Del vector operator
$\nabla^2$	Laplacian scalar operator
$C_0$	longitudinal wave velocity of the elementary theory
$C_1$	velocity of dilatational waves in an infinite elastic solid
$C_2$	velocity of distortional waves in an infinite elastic solid
$A$	cross-sectional area

LIST OF SYMBOLS (Continued)

<u>Symbol</u>	<u>Definition</u>
v	volume
a	radius of bar
ℓ	length of bar
L	wavelength of wave
η	wave number
K, K <sub>1</sub>	constants introduced into stress equations
R	radial stress at the surface of the bar
Z	shear stress at the surface of the bar
τ	ratio of thermoelastic velocity to elastic velocity
C	wave velocity in general
α	coefficient of volumetric thermal expansion
C <sub>e</sub>	specific heat at constant strain
Q	interval heat addition
k	thermal conductivity
ω	frequency
ε	thermoelastic material constant
K <sub>T</sub>	thermoelastic bulk modulus
q	thermoelastic damping coefficient
ω*	characteristic frequency
X	reduced frequency
ξ	reduced wave length
c, d	thermoelastic material constants

LIST OF SYMBOLS (Continued)

<u>Symbol</u>	<u>Definition</u>
$\beta$	thermoelastic wave parameter
i	imaginary number
<u>Subscripts</u>	
real	real portion of a complex quantity
imag	imaginary portion of a complex quantity

## INTRODUCTION

The purpose of this report is to ascertain the effects of thermoelastic damping on the propagation of longitudinal waves in cylindrical rods.

As a wave propagates down the length of a rod, the variation of compressional strain in the medium generates a small amount of heat flow which increases the entropy of the bar and dissipates a portion of the wave energy. This process is referred to as thermoelastic damping. In the past history of the development of solid mechanics, the magnitude of thermoelastic damping was considered extremely small. Therefore, emphasis was placed upon elastic wave propagation while thermal wave propagation was studied by thermodynamicists in terms of the heat transfer problem. Only recently, starting in the late 1950's, has the coupling of the thermal and elastic waves been considered. Thermoelastic wave propagation has been studied mainly for extended solids by H. Deresiewicz (1957) and by Chadwick and Sneddon (1958) and in a review article by Chadwick (1960), which also covers bounded solids. In particular, Chadwick extended the Pochhammer-Chree (1886) analysis of longitudinal elastic wave propagation in infinite circular rods to the thermoelastic case.

However, the Pochhammer-Chree elastic solution and the Chadwick thermoelastic extension are unnecessarily complicated for present engineering applications and therefore present a problem to which

this report is addressed, namely, an engineering understanding of thermoelastic wave propagation and damping.

The approach to this problem taken in this report is to find a satisfactory engineering approximation for elastic waves and then extend that solution to incorporate the coupling due to the thermal wave.

The literature abounds with engineering solutions of elastic wave propagation. Several of these methods are reviewed in Chapter II, and a particularly simple one-dimensional solution by Bishop (1952) is chosen as a basis for further work. A further correction to the Bishop approximation is developed to conform closely to experimental data.

In Chapter III, an energy equation consistent with the assumptions used in the elastic wave equation, coupled with the elastic equation of motion, is derived and is solved for the thermoelastic phase velocity and attenuation coefficient.

Several interesting cases are solved numerically. These solutions indicate that the effects of thermoelastic damping are very important at extremely high frequencies.

## CHAPTER I

### WAVE PROPAGATION IN AN INFINITE ELASTIC SOLID

#### A. The Equations of Motion

The equations of motion of an isotropic elastic medium are derived from basic principles in terms of cylindrical coordinates which were chosen in view of later applications to cylindrical rods. Starting with the stress component equations of motion and with the strain components in terms of particle displacements, the displacement equations of motion are derived using Hooke's law. These equations are then shown to correspond to two types of elastic wave propagation in an unbounded solid. The first type consists of a volumetric expansion-contraction wave front called a dilatation wave. The particle motion in this wave is along the direction of propagation. The second type of wave is commonly referred to as a distortional wave. Particle motion in a plane distortional wave takes place perpendicular to the direction of propagation. In an unbounded solid, only these two types of wave are propagated.

Figure 1 defines the cylindrical coordinate system along with the usual Cartesian coordinate system. The material of the rod is considered homogeneous and the section is in dynamic equilibrium under the influence of stresses and resulting accelerations. Displacements from the equilibrium condition are  $U$  along the radial coordinate  $r$ ,  $V$  along the angular coordinate  $\theta$ , and  $W$  along the

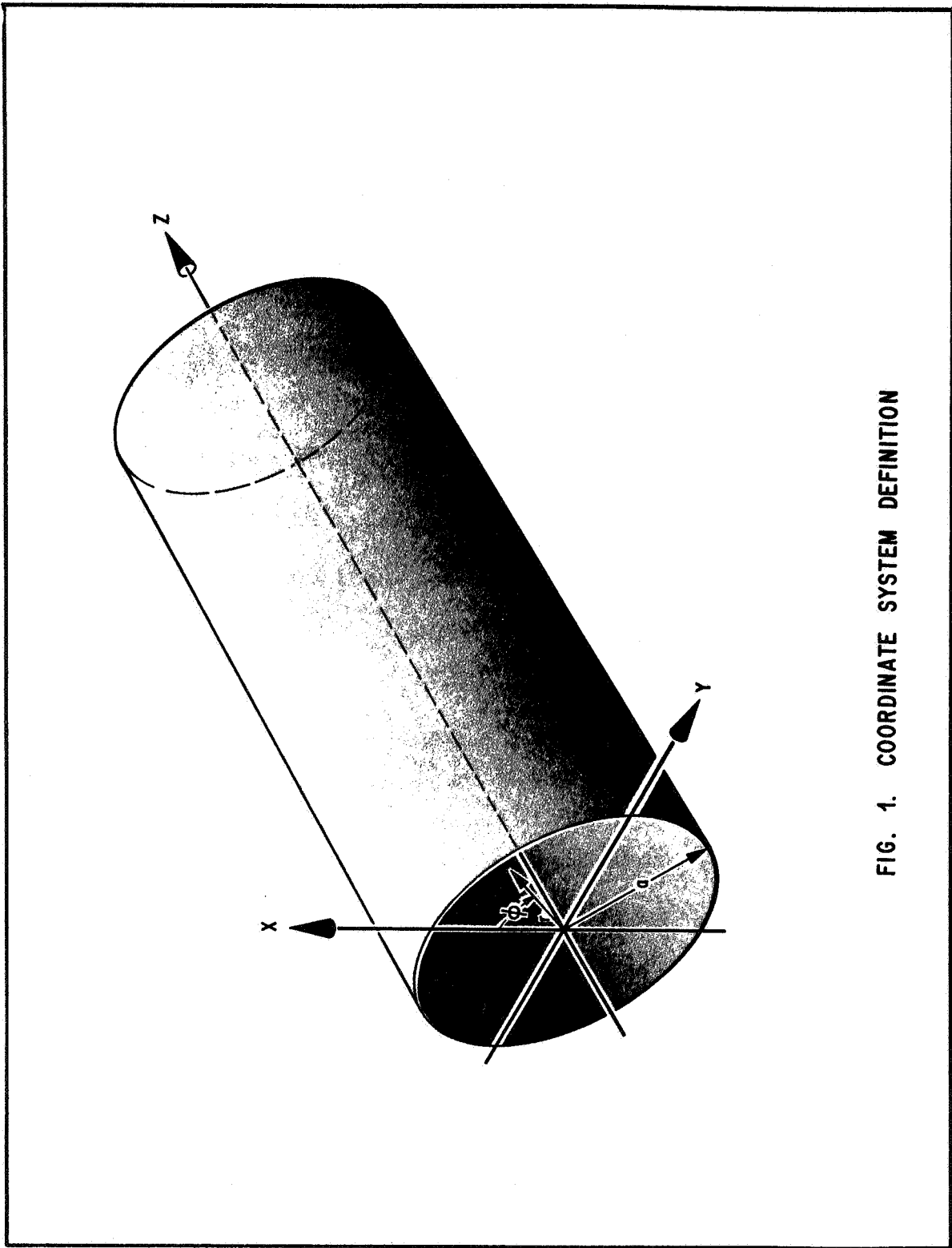


FIG. 1. COORDINATE SYSTEM DEFINITION

longitudinal coordinate  $z$ . The normal stresses are denoted by  $\sigma_r$ ,  $\sigma_\theta$ , and  $\sigma_z$ , and the shearing stresses are represented by  $\tau_{r\theta}$ ,  $\tau_{rz}$ , and  $\tau_{\theta z}$ . The mass per unit volume is  $\rho$ . The stress equations of motion for an elemental volume are

$$\frac{\partial \sigma_r}{\partial r} + \frac{1}{r} \frac{\partial \tau_{r\theta}}{\partial \theta} + \frac{\partial \tau_{rz}}{\partial z} + \frac{\sigma_r - \sigma_\theta}{r} = \rho \ddot{u} \quad (1a)$$

$$\frac{\partial \tau_{r\theta}}{\partial r} + \frac{1}{r} \frac{\partial \sigma_\theta}{\partial \theta} + \frac{\partial \tau_{\theta z}}{\partial z} + 2 \frac{\tau_{r\theta}}{r} = \rho \ddot{v} \quad (1b)$$

$$\frac{\partial \tau_{rz}}{\partial r} + \frac{1}{r} \frac{\partial \tau_{\theta z}}{\partial \theta} + \frac{\partial \sigma_z}{\partial z} + \frac{\tau_{rz}}{r} = \rho \ddot{w} \quad (1c)$$

Next, the strain-displacement relations are introduced. The normal strains are  $\epsilon_r$ ,  $\epsilon_\theta$ , and  $\epsilon_z$ , while the shearing strains are denoted by  $\gamma_{rz}$ ,  $\gamma_{r\theta}$ , and  $\gamma_{z\theta}$ . Thus, the strain displacement relationships are

$$\epsilon_r = \frac{\partial u}{\partial r} \quad (2a)$$

$$\epsilon_\theta = \frac{u}{r} + \frac{1}{r} \frac{\partial v}{\partial \theta} \quad (2b)$$

$$\epsilon_z = \frac{\partial w}{\partial z} \quad (2c)$$

$$\gamma_{r\theta} = \frac{1}{r} \frac{\partial u}{\partial \theta} + \frac{\partial v}{\partial r} - \frac{v}{r} \quad (2d)$$

$$\gamma_{z\theta} = \frac{1}{r} \frac{\partial w}{\partial \theta} + \frac{\partial v}{\partial z} \quad (2e)$$

$$\gamma_{rz} = \frac{\partial w}{\partial r} + \frac{\partial u}{\partial z} \quad (2f)$$

Adding the normal strain components yields the dilatation

$$\Delta = \frac{1}{r} \frac{\partial(rU)}{\partial r} + \frac{1}{r} \frac{\partial V}{\partial \theta} + \frac{\partial W}{\partial z} . \quad (3)$$

Also useful in later derivations are the rotations  $\bar{\omega}_r$ ,  $\bar{\omega}_\theta$ ,  $\bar{\omega}_z$  defined by

$$2\bar{\omega}_r = \frac{1}{r} \frac{\partial W}{\partial \theta} - \frac{\partial V}{\partial z} \quad (4a)$$

$$2\bar{\omega}_\theta = \frac{\partial U}{\partial z} - \frac{\partial W}{\partial r} \quad (4b)$$

$$2\bar{\omega}_z = \frac{1}{r} \left[ \frac{\partial(rV)}{\partial r} - \frac{\partial U}{\partial \theta} \right] . \quad (4c)$$

Within an isotropic, homogeneous material, each of the six components of stress at any point is a linear function of the six components of strain:

$$\sigma_r = \lambda\Delta + 2\mu\epsilon_r \quad (5a)$$

$$\sigma_\theta = \lambda\Delta + 2\mu\epsilon_\theta \quad (5b)$$

$$\sigma_z = \lambda\Delta + 2\mu\epsilon_z \quad (5c)$$

$$\tau_{r\theta} = \mu\gamma_{r\theta} \quad (5d)$$

$$\tau_{rz} = \mu\gamma_{rz} \quad (5e)$$

$$\tau_{z\theta} = \mu\gamma_{z\theta} , \quad (5f)$$

where  $\lambda$  and  $\mu$  are Lamé's constants defined below. Poisson's ratio is denoted by  $\nu$ , and Young's modulus is  $E$ .

$$\mu = \frac{E}{2(1 + \nu)} \quad (6)$$

$$\lambda = \frac{\nu E}{(1 + \nu)(1 - 2\nu)} \quad (7)$$

The displacement equations of motion are derived from the stress equations of motion (1) by introducing the stress-strain relations (5). After the appropriate substitution of various derivatives of the stress-strain equations and algebraic manipulations, an intermediate form of the equations of motion can be written:

$$\begin{aligned} (\lambda + \mu) \left[ \frac{\partial^2 U}{\partial r^2} + \frac{1}{r} \frac{\partial U}{\partial r} - \frac{U}{r^2} + \frac{1}{r} \frac{\partial^2 V}{\partial r \partial \theta} - \frac{1}{r^2} \frac{\partial V}{\partial \theta} + \frac{\partial^2 W}{\partial r \partial z} \right] \\ + \mu \frac{1}{r} \left[ \frac{\partial U}{\partial r} + \frac{\partial^2 U}{\partial r^2} + \frac{1}{r^2} \frac{\partial^2 U}{\partial z^2} \right] - \frac{\mu}{r^2} \left( U + 2 \frac{\partial V}{\partial \theta} \right) = \rho \ddot{U} \end{aligned} \quad (8a)$$

$$\begin{aligned} \left( \frac{\lambda + \mu}{r} \right) \left[ \frac{\partial^2 U}{\partial r \partial \theta} + \frac{1}{r} \frac{\partial U}{\partial \theta} + \frac{1}{r} \frac{\partial^2 V}{\partial \theta^2} + \frac{\partial^2 V}{\partial \theta \partial z} \right] + \mu \left[ \frac{1}{r} \frac{\partial V}{\partial r} + \frac{\partial^2 V}{\partial r^2} + \frac{1}{r^2} \frac{\partial^2 V}{\partial \theta^2} + \frac{\partial^2 V}{\partial z^2} \right] \\ + \frac{\mu}{r^2} \left( 2 \frac{\partial U}{\partial \theta} - V \right) = \rho \ddot{V} \end{aligned} \quad (8b)$$

$$\begin{aligned} (\lambda + \mu) \left[ \frac{\partial^2 U}{\partial r \partial z} + \frac{1}{r} \frac{\partial U}{\partial z} + \frac{1}{r} \frac{\partial^2 V}{\partial \theta \partial z} + \frac{\partial^2 W}{\partial z^2} \right] + \mu \left[ \frac{1}{r} \frac{\partial W}{\partial r} + \frac{\partial^2 W}{\partial r^2} + \frac{1}{r^2} \frac{\partial^2 W}{\partial \theta^2} + \frac{\partial^2 W}{\partial z^2} \right] = \rho \ddot{W}. \end{aligned} \quad (8c)$$

The first terms of these equations can be recognized as the partial derivatives of the dilatation  $\Delta$  with respect to  $r$ ,  $\theta$ , and  $z$ . The second terms can be shown to be the Laplacian of  $U$ ,  $V$ , and  $W$  in cylindrical coordinates. The Laplacian in cylindrical coordinates is

$$\nabla^2 = \frac{\partial}{\partial r^2} + \frac{1}{r} \frac{\partial}{\partial r} + \frac{1}{r^2} \frac{\partial}{\partial \theta^2} + \frac{\partial^2}{\partial z^2} . \quad (9)$$

Thus, the equations of motion (8) can be simplified:

$$(\lambda + \mu) \frac{\partial \Delta}{\partial r} + \mu \nabla^2 U - \frac{\mu}{r^2} (U + 2 \frac{\partial V}{\partial \theta}) = \rho \ddot{U} \quad (10a)$$

$$\frac{(\lambda + \mu)}{r} \frac{\partial \Delta}{\partial \theta} + \mu \nabla^2 V + \frac{\mu}{r^2} (2 \frac{\partial U}{\partial \theta} - V) = \rho \ddot{V} \quad (10b)$$

$$(\lambda + \mu) \frac{\partial \Delta}{\partial z} + \mu \nabla^2 W = \rho \ddot{W}. \quad (10c)$$

As a basis for further development, these equations are recast by using the derivation of the rigid body rotations  $\bar{\omega}_r$ ,  $\bar{\omega}_\theta$ , and  $\bar{\omega}_z$  of equation (4) and by manipulating equation (8). The equations of motion in this form are known as the Pochhammer-Chree equations:

$$(\lambda + 2\mu) \frac{\partial \Delta}{\partial r} - \frac{2\mu}{r} \frac{\partial \bar{\omega}_z}{\partial \theta} + 2\mu \frac{\partial \bar{\omega}_\theta}{\partial z} = \rho \ddot{U} \quad (11a)$$

$$\frac{(\lambda + 2\mu)}{r} \frac{\partial \Delta}{\partial \theta} - 2\mu \frac{\partial \bar{\omega}_r}{\partial z} + 2\mu \frac{\partial \bar{\omega}_z}{\partial r} = \rho \ddot{V} \quad (11b)$$

$$(\lambda + 2\mu) \frac{\partial \Delta}{\partial z} - \frac{2\mu}{r} \frac{\partial}{\partial r} (r \bar{\omega}_\theta) + \frac{2\mu}{r} \frac{\partial \bar{\omega}_r}{\partial \theta} = \rho \ddot{W}. \quad (11c)$$

## B. Wave Propagation

The Pochhammer-Chree equations allow the determination of the propagation of two types of wave motion.

Manipulation of equations (11) results in the wave equation

$$\rho \frac{\partial^2 \Delta}{\partial t^2} = (\lambda + 2\mu) \nabla^2 \Delta, \quad (12)$$

in its most general form. This equation shows that the dilatation  $\Delta$  is propagated throughout the elastic medium with a velocity

$$c_1 = \left[ \frac{(\lambda + 2\mu)}{\rho} \right]^{1/2}. \quad (13)$$

More strictly, this wave should be termed irrotational.

By differentiating (11b) with respect to  $z$ , and by subtracting a multiple of the differential of (11c) with respect to  $\theta$ , the following form appears

$$\frac{\partial^2 \bar{\omega}_r}{\partial t^2} = \frac{\mu}{\rho} \nabla^2 \bar{\omega}_r. \quad (14)$$

Similar equations can likewise be obtained for  $\bar{\omega}_\theta$  and  $\bar{\omega}_z$ . Thus, it has been shown that the rotational wave form is propagated with a velocity

$$c_2 = [\mu/\rho]^{1/2}. \quad (15)$$

The strict term for this wave is equivoluminal; however, the more popular term is distortional or shear wave.

It has thus been shown that, in an elastic solid, waves may be propagated with a velocity  $C_1$  for waves involving no rotation and with velocity  $C_2$  for waves involving no dilatation travel. The velocity designations,  $C_1$  and  $C_2$ , are used for consistency with published literature.

These results will be applied when the effects of the stress conditions at the solid boundary are introduced and the concept of dispersion is revealed.

## CHAPTER II

### LONGITUDINAL ELASTIC WAVE PROPAGATION IN CYLINDRICAL RODS

#### A. Elementary Theory

It is possible, at least theoretically, to derive the propagation of stress waves in any bounded isotropic solid by solving the displacement equations of motion for the appropriate boundary conditions. In fact, because of the reflection of plane elastic waves at free surfaces and because of the extremely complicated fashion in which the dilatational and distortional waves are reflected as they travel up and down the bar, no exact solutions have been obtained. Thus, introducing boundary conditions into the equations of motion produces dispersion; that is, the velocity of wave propagation of a disturbance up and down the bar is a function of wavelength.

The governing equations have been approximated by many in the field of elasticity. These approximations reduce to either of two types. The first introduces approximations into the equation of motion, while the second uses the exact equations of motion and only approximately satisfies the boundary conditions. The first method has been chosen for review and extension.

Basically, three types of wave motion occur in thin rods: longitudinal, torsional, and lateral. In longitudinal motion, the elements of the rod extend and contract, but there is no lateral or transverse

motion of the axis of the rod. In torsional motion, each transverse section of the bar remains in its own plane and rotates about its center; again the axis of the rod is undisturbed. Lateral waves correspond to bending of the rod, and elements of the bar axis move laterally during the motion.

Only longitudinal wave motion will be considered in this report. Historically speaking, the first treatment of longitudinal wave motion neglected the radial displacements arising from Poisson's effect. As a result, this first treatment predicted a wave velocity independent of frequency. A second elementary treatment was introduced by Lord Rayleigh, who shows that, by including the effect of radial inertia, the wave propagation velocity is a function of wavelength. These and further investigations, including the effects of radial shear by Mindlin and Herrmann and by Bishop, are compared in this chapter.

The elementary theory of longitudinal wave propagation in a cylindrical rod assumes that the cross-sectional element faces remain plane and that the stress distribution is constant across the faces. Thus, the equation of motion can be directly written. Using Newton's law and introducing the material density  $\rho$  and forces due to the stresses on both sides of the element, we can write

$$\rho \frac{\partial^2 W}{\partial t^2} = \frac{\partial \sigma_z}{\partial z} . \quad (16)$$

By ignoring the lateral contraction due to longitudinal strain, we obtain

$$\sigma_z = E \frac{\partial W}{\partial z} . \quad (17)$$

Thus, the equation of motion can be written

$$\frac{\partial^2 W}{\partial t^2} = \frac{E}{\rho} \frac{\partial^2 W}{\partial z^2} . \quad (18)$$

Equation (18) is the classical first approximation for longitudinal wave motion in a rod. The velocity of propagation is

$$C_0 = [E/\rho]^{1/2} . \quad (19)$$

The designation " $C_0$ " is used in the literature to distinguish it from the dilatational and shear velocities,  $C_1$  and  $C_2$ . Notice, however, that the elementary treatment assumes that the plane transverse sections remain plane during the stress wave passage and that stress is uniform across the plane section. However, we know that longitudinal contractions and expansions will result in lateral expansions and contractions. The resulting lateral motion will cause non-uniform distribution of stress across the section of the bar, and plane transverse sections become distorted. The lateral effects will be small, however, when the wavelength of the wave is very much larger than the diameter of the bar. Thus we would expect any detailed analysis of longitudinal vibrations to reduce to the wave velocity  $C_0$  for very small ratios of the bar diameter to the wavelength.

## B. Rayleigh-Love Correction

The next important development in wave propagation in elastic rods was made by considering lateral contraction due to longitudinal strains. This was first published by Lord Rayleigh (John William Strutt) in 1877 and later by A. E. H. Love. Rayleigh's derivation was based on the principle that a frequency of free vibration of a conservative system can be obtained by equating the time average of the potential and kinetic energies of the motion. Love used Hamilton's principle in obtaining the equations of motion. The derivation used in this report will be developed from the displacement equations of motion.

Because the rod is axisymmetric, the normal strain equations (2a), (2b), and (2c) simplify to:

$$\epsilon_r = \frac{\partial U}{\partial r} \quad (20a)$$

$$\epsilon_\theta = \frac{U}{r} \quad (20b)$$

$$\epsilon_z = \frac{\partial W}{\partial z} \quad (20c)$$

The shear strain equations are all zero by virtue of axisymmetry and an assumed independence of  $z$  upon  $U$ .

The radial strain  $\epsilon_r$  simply is Poisson's ratio  $\nu$  times the longitudinal strain  $\epsilon_z$ . Substituting equations (20a), (20b) and (20c) into the strain relations, and integrating with respect to  $r$  yield:

$$U = - \nu r \frac{\partial W}{\partial z} . \quad (21)$$

Thus, equation (20b) becomes

$$\epsilon_{\theta} = - \nu \frac{\partial W}{\partial z} . \quad (22)$$

Now substitution of the above statements into the stress strain equations (5) yields

$$\sigma_r = \lambda \Delta - 2\mu \nu \frac{\partial W}{\partial z} \quad (23a)$$

$$\sigma_{\theta} = \lambda \Delta - 2\mu \nu \frac{\partial W}{\partial z} \quad (23b)$$

$$\sigma_z = \lambda \Delta - 2\mu \frac{\partial W}{\partial z} . \quad (23c)$$

These equations are then substituted into the radial equation of motion (1a) which is then solved for the partial of radial stress with respect to r:

$$\frac{\partial \sigma_r}{\partial r} = - \nu r \rho \frac{\partial^3 W}{\partial z \partial t^2} . \quad (24)$$

Integration (24) with respect to r from 0 to r yields the radial stress:

$$\tilde{\sigma}_r = \nu \rho \frac{\partial^2 W}{\partial z \partial t^2} \frac{r^2}{2} . \quad (25)$$

Using equation (5) and the foregoing statements yields:

$$E \frac{\partial W}{\partial z} = \sigma_z - v^2 r^2 \rho \frac{\partial^2 W}{\partial z \partial t^2} . \quad (26)$$

Equation (23) is solved for the partial of longitudinal stress with respect to  $z$ , and is then integrated over the cross-sectional area of the bar to yield

$$\frac{\partial \sigma_z}{\partial z} = E \frac{\partial^2 W}{\partial z^2} + \frac{v^2 a^2 \rho}{2} \frac{\partial^4 W}{\partial z \partial t^2} . \quad (27)$$

Equation (27), substituted into the axial equation of motion (1c), results in the wave equation

$$\frac{E}{\rho} \frac{\partial^2 W}{\partial z^2} + \frac{v^2 a^2}{2} \frac{\partial^2 W}{\partial z^2 \partial t^2} = \frac{\partial^2 W}{\partial t^2} . \quad (28)$$

A solution of this partial differential equation is

$$W = e^{i\eta(z-Ct)} , \quad (29)$$

where  $\eta = \frac{2\pi}{L}$ , and  $L$  is the wavelength. The velocity of wave propagation is then

$$C = C_0 \left[ 1 + \frac{\eta^2 v^2 a^2}{2} \right]^{1/2} . \quad (30)$$

Thus, we see that the velocity of wave propagation is a function of the wavelength, known as "configurational dispersion." For long waves the wave speed is  $C_0$ , corresponding to the elementary theory. However,

equation (30) predicts zero wave velocity at zero wavelength. This is not borne out by experimental investigations, which show the wave velocities for short wavelengths to approach the surface wave velocity first discovered by Rayleigh.

### C. Mindlin and Herrmann's Method

Mindlin and Herrmann's method for longitudinal wave propagation in a cylindrical rod proceeds from the displacements:

$$U = \frac{r}{a} U(z, t) \quad (31a)$$

$$V = 0 \quad (31b)$$

$$W = W(z, t), \quad (31c)$$

which are then substituted into an incremental energy equation

$$\Delta U = \int_t dt \int_v \frac{\partial}{\partial t} (T - V) dv, \quad (32)$$

and integrated over the cross section. The four resulting bar stresses are then removed by integrating the stress equations of motion over the radius of the section and by using Hooke's law to convert the stress equations of motion into displacement equations. To make the wave velocities fit the exact theory, the constants  $K$  and  $K_1$  are then introduced into the displacement equations. The resulting displacement equations consist of two coupled partial differential equations:

$$a^2 K_1^2 \mu^2 \frac{\partial^2 U}{\partial z^2} - 8K_1^2 (\lambda + \mu) U - 4aK_1^2 \lambda \frac{\partial W}{\partial z} + 4aR = \rho a^2 \frac{\partial^2 U}{\partial t^2} \quad (33a)$$

and

$$2a\lambda \frac{\partial U}{\partial z} + a^2 (\lambda + 2\mu) \frac{\partial^2 W}{\partial z^2} + 2aZ = \rho a^2 \frac{\partial^2 W}{\partial t^2}, \quad (33b)$$

where

$$R = \left. \sigma_r \right|_{r=a} \quad \text{and} \quad Z = \left. \tau_{zr} \right|_{r=a}. \quad (33c)$$

Mindlin and Herrmann assume the solutions to these equations to be:

$$U = Ae^{i\eta(z-Ct)} \quad (34a)$$

$$W = Be^{i\eta(z-Ct)} \quad (34b)$$

$$R = Z = 0. \quad (34c)$$

As a result the dispersion equation was written as

$$\left[ \frac{K^2 \mu}{\rho} + \frac{8K_1^2 (\lambda + \mu)}{a^2 \eta^2 \rho} - c^2 \right] \left[ \frac{\lambda + 2\mu}{\rho} - c^2 \right] - \frac{8K_1^2 \lambda^2}{a^2 \eta^2 \rho^2} = 0. \quad (35)$$

This equation represents two modes of wave propagation in the bar.

For long wavelengths, the wave velocities are

$$c^2 = \frac{E}{\rho} = c_0^2, \quad (36a)$$

and

$$c^2 \rightarrow \infty. \quad (36b)$$

The first branch (equation (36a)) agrees with the elementary theory.

For short wavelengths, the wave velocities are

$$C^2 = K^2 \frac{\mu}{\rho}, \quad (37a)$$

and

$$C^2 = \frac{\lambda + 2\mu}{\rho}. \quad (37b)$$

The first parameter  $K^2$  is used to fit the dispersion curve to the Rayleigh surface wave velocity. The second parameter  $K_1^2$  is used to fit the dispersion curve to the Pochhammer-Chree curve at a common point  $C^2 = 2C_2^2$  for all values of Poisson's ratio  $\nu$ . The coupled equations of motion (33a) and (33b) are then written to eliminate  $U$ .

$$\begin{aligned} \frac{E}{\rho} \frac{\partial^2 W}{\partial z^2} - \frac{\partial^2 W}{\partial t^2} + \frac{2Z}{\rho a} + \frac{\rho a^2}{8K_1^2(\lambda + \mu)} \frac{\partial^2}{\partial t^2} \left[ \frac{(\lambda + 2\mu)}{\rho} \frac{\partial^2 W}{\partial z^2} + \frac{2Z}{\rho a} - \frac{\partial^2 W}{\partial t^2} \right] \\ - \frac{a^2 K^2 \mu}{8K_1^2(\lambda + \mu)} \frac{\partial^2}{\partial t^2} \left[ \frac{(\lambda + 2\mu)}{\rho} \frac{\partial^2 W}{\partial z^2} - \frac{\partial^2 W}{\partial t^2} + \frac{2Z}{\rho a} \right] + \frac{\lambda}{\rho K_1^2(\lambda + \mu)} \frac{R}{z} = 0 \end{aligned} \quad (38)$$

Inspection of equation (38) shows that Mindlin and Herrmann's method improves the Rayleigh-Love differential equation by adding the radial shear effect and by improving the radial inertia term.

#### D. Bishop's Method

Bishop's original paper on the velocity of wave propagation in circular elastic rods was prepared in 1952 in an effort to improve the prediction of elastic wave propagation velocity as a function of wavelength. Bishop derived an approximation to the equations of

motion in Cartesian coordinates including the lateral inertia as Rayleigh and Love and also an approximation to the lateral shear stress. He used a theorem relating to convex boundaries to remove geometric problems in describing the cross sectional boundary. However, for clarity, we shall use Hamilton's principle and cylindrical coordinates to derive the equation of motion.

The strain relations for  $\epsilon_r$ ,  $\epsilon_\theta$ , and  $\epsilon_z$  are the same as that of Rayleigh and Love. Unlike Rayleigh and Love, Bishop did not ignore the shear strain.

$$\gamma_{rz} = \frac{\partial U}{\partial z} = -r \frac{\partial^2 W}{\partial z^2} . \quad (39)$$

Hamilton's principle states that the first variation of the time integral of kinetic energy minus the potential energy during a process is zero, as symbolically stated below:

$$\delta \int_t (T - V) dt = 0. \quad (40)$$

The strain potential energy of an elastic material (per unit volume) is the integral of the elastic force over the displacement

$$V = \int F dz \quad (41)$$

where

$$F = Ez. \quad (42)$$

Integrating from zero to  $\epsilon_z$  results in the strain energy per unit volume of

$$V = 1/2 E \epsilon_z^2. \quad (43)$$

Likewise, the shearing strain energy is

$$V = 1/2 \mu \gamma_{rz}^2. \quad (44)$$

Thus, the total potential energy is

$$V = 1/2 \int_0^r \int_0^\theta \int_0^z (E \epsilon_z^2 + \mu \gamma_{rz}^2) r dr d\theta dz, \quad (45)$$

or, for the rod in question,

$$V = \pi \int_0^r \int_0^z (E \epsilon_z^2 + \mu \gamma_{rz}^2) r dr dz. \quad (46)$$

Substitution of the strain relations yields

$$V = \pi \int_0^r \int_0^z \left[ E (\partial W / \partial z)^2 + \mu v^2 r^2 \left( \frac{\partial^2 W}{\partial z^2} \right)^2 \right] r dr dz. \quad (47)$$

The kinetic energy per unit volume is

$$T = 1/2 \rho \left[ (\partial U / \partial t)^2 + (\partial W / \partial t)^2 \right]. \quad (48)$$

Substituting the strain relations and integrating, we obtain

$$T = \rho\pi \int_0^r \int_0^z \left[ \nu^2 r^2 \left( \frac{\partial^2 W}{\partial z \partial t} \right)^2 + (\partial W / \partial t)^2 \right] r dr dz. \quad (49)$$

When we substitute these forms into Hamilton's equation and integrate over the cross section of the bar, we obtain (introducing subscript notation for partial derivatives)

$$\delta \int_{t_1}^{t_2} \int_{z=0}^{\ell} \frac{\pi a^2}{2} \left[ \rho \nu^2 \frac{a^2}{2} (W_{zt})^2 + \rho (W_t)^2 - E (W_z)^2 - \mu \nu^2 \frac{a^2}{2} (W_{zz})^2 \right] dz dt = 0. \quad (50)$$

Forming the functional

$$F = \frac{\pi a^2}{2} \left[ \rho \nu^2 \frac{a^2}{2} (W_{zt})^2 + \rho (W_t)^2 - E (W_z)^2 - \mu \nu^2 \frac{a^2}{2} (W_{zz})^2 \right], \quad (51)$$

and using the Euler-Lagrange necessary condition of the variational calculus, we obtain

$$\begin{aligned} \frac{\partial F}{\partial W} - \frac{\partial}{\partial z} \left( \frac{\partial F}{\partial W_z} \right) - \frac{\partial}{\partial t} \left( \frac{\partial F}{\partial W_t} \right) + \frac{\partial^2}{\partial z^2} \left( \frac{\partial F}{\partial W_{zz}} \right) + \frac{\partial^2}{\partial t^2} \left( \frac{\partial F}{\partial W_{tt}} \right) \\ + \frac{\partial^2}{\partial z \partial t} \left( \frac{\partial F}{\partial W_{zt}} \right) = 0. \end{aligned} \quad (52)$$

After we form and substitute the indicated partial derivatives, the resulting equation of motion is

$$\frac{E}{\rho} W_{zz} - \frac{uv^2a^2}{2\rho} W_{zzzz} + \frac{v^2a^2}{2} W_{zztt} = W_{tt}. \quad (53)$$

By noting the elementary propagation velocity,  $C_0$ , and the distortional wave velocity in an extended medium,  $C_2$ , we can simplify equation (53):

$$C_0^2 W_{zz} - C_2^2 \frac{v^2a^2}{2} W_{zzzz} + \frac{v^2a^2}{2} W_{zztt} = W_{tt}. \quad (54)$$

Again, assuming a solution

$$W = e^{i\eta(z-Ct)}, \quad (55)$$

yields the dispersion equation

$$C^2 \left[ 1 + \frac{v^2a^2\eta^2}{2} \right] - \left[ C_0^2 + \frac{v^2a^2\eta^2}{2} C_2^2 \right] = 0. \quad (56)$$

For long wavelengths ( $\eta$  approaches zero), the wave velocity is the same as that for the elementary theory. For short wavelengths ( $\eta$  approaches infinity), the velocity of wave propagation approaches the velocity of shear (distortional) waves in an infinite medium. Thus, we observe, by comparing equation (56) with equation (30), that Bishop's contribution is the addition of the radial shear term to the Rayleigh-Love analysis.

### E. Comparison of Bishop's Method and Mindlin and Herrmann's Method

Comparison of the results of these two methods begins by comparing their dispersion curves with numerical approximations to the Pochhammer-Chree equations by Bancroft and Hudson in figure 2. It can be noted that both the Bishop and the Herrmann and Mindlin dispersion equations result in wave velocities greater than the Pochhammer-Chree numerical solutions for all wavelengths. However, the errors resulting from the Mindlin and Herrmann method are generally smaller, due in fact to the use of the constants  $K$  and  $K_1$  for curve fitting. For our purpose an insight into the complexity of the Mindlin and Herrmann method can be gained from a comparison of the equations of motion of the methods.

Using Mindlin and Herrmann's one-dimensional equation of motion (38) and assuming that

$$W = B e^{i\eta(z-Ct)} \quad (57a)$$

and

$$R = Z = 0, \quad (57b)$$

we obtain the following form:

$$\begin{aligned} \frac{E}{\rho} W_{zz} - W_{tt} + \frac{a^2}{8K_1^2(\lambda + \mu)} \left[ (\lambda + 2\mu) + K^2\mu \right] W_{ttzz} \\ - \frac{\rho a^2}{8K_1^2(\lambda + \mu)} W_{tttt} - \frac{a^2 K^2 \mu (\lambda + 2\mu)}{8K_1^2(\lambda + \mu) \rho} W_{zzzz} = 0 \end{aligned} \quad (58)$$

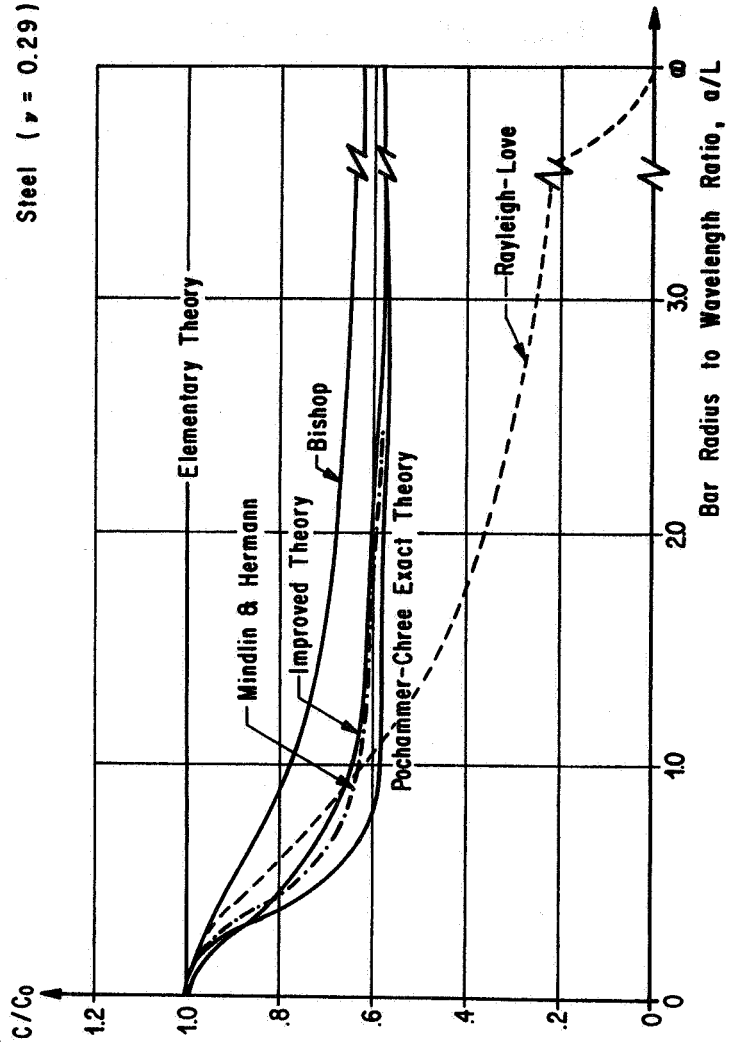


FIG. 2. LONGITUDINAL ELASTIC WAVE PROPAGATION VELOCITY AS A FUNCTION OF RADIUS TO WAVELENGTH RATIO

which is to be compared with Bishop's equation of motion (53)

$$\frac{E}{\rho} W_{zz} - W_{tt} + \frac{v^2 a^2}{2} W_{ttzz} - \frac{v^2 a^2 \mu}{2\rho} W_{zzzz} = 0. \quad (59)$$

#### F. Improved Longitudinal Wave Equation

The simple form of the Bishop equation of motion suggests its use in an improved form as an engineering tool. The basic equations of motion are reformulated here in terms of the stress equations with constants  $K$  and  $K_1$  used to fit the resulting dispersion curve to the numerical solution of the Pochhammer-Chree equations.

Starting with the stress-strain relationships of the Rayleigh-Love analysis (equation (23)) and the shear strain relation of the Bishop analysis (equation (39))

$$\sigma_r = \lambda \Delta - 2\mu\nu \frac{\partial W}{\partial z} \quad (60a)$$

$$\sigma_\theta = \lambda \Delta - 2\mu\nu \frac{\partial W}{\partial z} \quad (60b)$$

$$\sigma_z = \lambda \Delta - 2\mu\nu \frac{\partial W}{\partial z} \quad (60c)$$

$$\tau_{rz} = -\mu\nu r \frac{\partial^2 W}{\partial z^2} \quad (60d)$$

and substituting into the radial stress equations of motion (equation (1a)), we obtain the following:

$$\frac{\partial \sigma_r}{\partial r} = K^2 \mu\nu r \frac{\partial^3 W}{\partial z^3} - K_1^2 \nu r \rho \frac{\partial^3 W}{\partial z \partial t^2}. \quad (61)$$

Integrating equation (61) with respect to  $r$  yields

$$\sigma_r = - \frac{K^2 \mu \nu r^2}{2} \frac{\partial^3 W}{\partial z^3} + \frac{K_1^2 \nu \rho r^2}{2} \frac{\partial^3 W}{\partial z \partial t^2}. \quad (62)$$

Now using equation (59c) and the strain equation (2) and taking the derivative with respect to  $z$  yields

$$\frac{\partial \sigma}{\partial z} = E \frac{\partial^2 W}{\partial z^2} - K^2 \mu \nu^2 r^2 \frac{\partial^4 W}{\partial z^4} + K_1^2 \nu^2 \rho r^2 \frac{\partial^4 W}{\partial z^2 \partial t^2}. \quad (63)$$

After we integrate over the cross section and divide by the cross-sectional area to find the total bar stress, and when we substitute into the classical bar stress equation of motion (equation (16)), we have the improved wave equation written with previous notations:

$$C_0^2 \frac{\partial^2 W}{\partial z^2} - K^2 C_2^2 \frac{\nu^2 a^2}{2} \frac{\partial^4 W}{\partial z^4} + K_1^2 \frac{\nu^2 a^2}{2} \frac{\partial^4 W}{\partial z^2 \partial t^2} - \frac{\partial^2 W}{\partial t^2} = 0. \quad (64)$$

Introducing the solution

$$W = e^{i\eta(z-Ct)} \quad (65)$$

yields the dispersion equation

$$-C_0^2 + C^2 \left[ 1 + \frac{K_1^2 \nu^2 a^2 \eta^2}{2} \right] - K^2 C_2^2 \frac{\nu^2 a^2 \eta^2}{2} = 0. \quad (66)$$

For long wavelengths ( $\eta \rightarrow 0$ ), the wave speed equals the elementary wave speed,  $C_0$ . For short wavelengths, the wave propagation velocity is

$$C^2 = \frac{K^2}{K_1^2} C_2^2. \quad (67)$$

The ratio of the constants can be used to fit the dispersion curve to the Rayleigh surface wave velocity. This ratio equals 92.6 percent of the shear (distortional wave velocity in an infinite medium for a Poisson's ratio of 0.29, which is typical of steel. Then, if the dispersion curve is fit at  $a/L = 0.293$  and  $C/C_2 = 2$ , as in Herrmann and Mindlin, the results can be plotted (see figure 2). Also shown for comparison are the Bishop curve and Mindlin and Herrmann curve (Pochhammer - Chree numerical solution by Hudson). Notice that the improved solution lies between the exact and Mindlin and Herrmann curves. Thus, we have a very simple improvement to the Bishop form of the longitudinal wave equation.

CHAPTER III  
THERMOELASTIC WAVES

A. Thermoelastic Equations of Motion

Chapter I reviews the basic principles of elastic wave propagation in an unbounded solid and Chapter II examines the characteristics of longitudinal wave propagation in cylindrical bars. This chapter discusses the salient points of thermal modification of longitudinal elastic waves.

When a longitudinal wave passes through a bar, any given element is compressed and extended. These volumetric changes are accompanied by heating and cooling. The heat generated during the compressional phase is conducted through the bar. The resulting temperature change affects the state of strain by the coefficient of thermal expansion.

The approach taken here is to combine these thermal effects with the improved wave equation developed in Chapter II. The resultant effects upon the purely elastic wave motion are discussed in terms of a change in the propagation velocity, and the addition of a damping effect upon the mechanical energy of the elastic wave due to heat conduction.

The thermally coupled case of longitudinal harmonic wave propagation is derived from the stress-displacement radial equation of motion developed for the improved elastic wave equation (62) coupled with the energy equation.

The thermoelastic stress-strain relationship is written:

$$\epsilon_r = \frac{1}{3}\alpha T + \frac{1}{E} [\sigma_r - \nu(\sigma_\theta + \sigma_z)] \quad (68)$$

where  $\alpha$  = coefficient of volumetric thermal expansion. By observing that  $\sigma_r$  equals  $\sigma_\theta$ , we write

$$\frac{\partial \sigma_z}{\partial z} = E \frac{\partial^2 W}{\partial z^2} - K^2 \mu^2 \nu^2 r^2 \frac{\partial^4 W}{\partial z^4} + K_1^2 \nu^2 \rho r^2 \frac{\partial^4 W}{\partial z^2 \partial t^2} - \frac{E\alpha}{3} \frac{\partial T}{\partial z}. \quad (69)$$

This equation is then integrated over the circular cross section to yield:

$$\frac{\partial \sigma_z}{\partial z} = E \frac{\partial^2 W}{\partial z^2} - K^2 \frac{a^2 \mu \nu^2}{2} \frac{\partial^4 W}{\partial z^4} + K_1^2 \frac{a^2 \nu^2 \rho^2}{2} \frac{\partial^4 W}{\partial z^2 \partial t^2} - \frac{E\alpha}{3} \frac{\partial T}{\partial z}. \quad (70)$$

Equation (68) is introduced into the stress equation of motion derived for the elementary case,

$$\frac{\partial \tilde{\sigma}_z}{\partial z} = \rho \frac{\partial^2 W}{\partial t^2}, \quad (71)$$

and, thus, the following equation of motion is obtained:

$$\frac{E}{\rho} W_{zz} - \frac{K^2 \nu^2 a^2 \mu}{2} W_{zzzz} + \frac{K_1^2 \nu^2 a^2}{2} W_{zztt} - \frac{E\alpha}{3\rho} T_z = W_{tt}. \quad (72)$$

The general form of the energy equation is written most often in the form

$$\frac{\alpha E T_0}{3(1-2\nu)} \frac{\partial(\text{div } \bar{U})}{\partial t} + \rho C_\epsilon \frac{\partial T}{\partial t} = K \nabla^2 T + Q, \quad (73)$$

where

$C_e$  = specific heat at constant strain

$\bar{U}$  = displacement vector

$Q$  = internal heat addition

and

$k$  = thermal conductivity.

But  $\text{div } \bar{U}$  is the dilatation  $\Delta$ , which is evaluated to be

$$\Delta = (1 - 2\nu) \frac{\partial W}{\partial z}. \quad (74)$$

The Laplacian of temperature,  $\nabla^2 T$ , is evaluated by assuming that the temperature gradient across the cross section is zero. Thus, the energy equation (with no internal heat generation) becomes

$$C_e \frac{\partial T}{\partial t} + \frac{E \alpha T}{3} W_{zt} = \frac{k}{\rho} T_{zz}. \quad (75)$$

Equations (72) and (75) are the coupled partial differential equations of thermoelastic disturbances in a cylindrical bar of infinite length. Because we wish to find thermoelastic damping attenuation coefficients, as well as phase velocity, solutions of the type

$$W = W_0 e^{i(\eta z - \omega t)} \quad (76a)$$

and

$$T = T_0 e^{i(\eta z - \omega t)} \quad (76b)$$

are most fitting. In general  $\omega$  and  $\eta$  are complex quantities. The wavelength of the plane harmonic waveform is  $2\pi/\omega_{\text{real}}$ .

Substituting equations (76) into (72) and (75) yields the two relations:

$$W_o \left( -\frac{E}{\rho} \eta^2 - \frac{K^2 v^2 a^2 \mu}{2\rho} \eta^4 + \frac{K_1^2 v^2 a^2}{2} \eta^2 \omega^2 + \omega^2 \right) = \frac{E \alpha T_o}{3\rho} i \eta \quad (77)$$

and

$$\frac{-T_o W_o E \alpha}{3} \eta \omega = T_o \left( \frac{k \eta^2}{\epsilon} - i \omega C_\epsilon \right). \quad (78)$$

Eliminating T and W and multiplying by  $-i/C_\epsilon$  yields the thermoelastic wave equation for longitudinal harmonic plane waves propagating in an infinite cylindrical rod

$$\left( \omega + i \frac{k \eta^2}{\rho C_\epsilon} \right) \left[ C_o^2 \eta^2 + \frac{K^2 a^2 \mu v^2}{2E} C_o^2 \eta^4 - \frac{K_1^2 v^2 a^2}{2} \eta^2 \omega^2 - \omega^2 \right] + \epsilon C_o^2 \omega \eta^2 = 0 \quad (79)$$

where

$$\epsilon = \frac{\alpha^2 T_o}{\rho^2 C_\epsilon K_T C_o^2}, \quad (80)$$

and

$$K_T = \frac{3}{E}. \quad (81)$$

If  $\omega$  is chosen as a real quantity representing waves of assigned frequency, the complex wave number  $\eta$  can be found as a function of frequency. By expanding the form in equation (76), we get

$$e^{i(\eta z - \omega t)} = e^{i[\eta_{\text{real}} + i\eta_{\text{imag}}] - \omega t} = e^{-\eta_{\text{imag}} z} \cos\left(z - \frac{\omega}{\eta_{\text{real}}} t\right). \quad (82)$$

Thus, the wave velocity equals  $\omega/\eta_{\text{real}}$ , and the attenuation coefficient  $q$  equals  $\eta_{\text{imag}}$ . Thus, the damping is a function of wave travel and is independent of time. Solutions of assigned wavelength can also be obtained from equation (79) but were not found due to the general interest of the assigned frequency solutions.

### B. Uncoupled Solution

The thermoelastic wave equation above consists of a pure thermal wave coupled through the constant  $\epsilon$  to the improved elastic wave equation found in the last chapter. Thus, when the coupling constant is zero, the thermal and elastic waves exist separately. If equation (79) is uncoupled ( $\epsilon = 0$ ), the solutions are

$$\eta_{\text{imag}}^2 = \frac{i\rho C}{k} \omega, \quad (83)$$

corresponding to the thermal mode, and

$$\eta_{\text{real}}^2 = \left[ \frac{\left( C_0^2 - \frac{K_1^2 v^2 a^2 \omega^2}{2} \right) \rho}{K^2 v^2 a^2 \mu} \left[ -1 \pm 1 + \frac{2K^2 v^2 a^2 \mu \omega^2}{\rho \left( C_0^2 - \frac{K_1^2 v^2 a^2 \omega^2}{2} \right)^2} \right]^{1/2} \right]^{1/2} \quad (84)$$

corresponding to the elastic mode. The phase velocity,  $V = \omega/\eta_{\text{real}}$ , is solved in terms of the wavelength  $L = 2\pi/\omega$  and yields

$$V^2 = \frac{C_0^2 \left[ 1 + \frac{2K^2 v^2 a^2 \pi^2}{L^2} \frac{C_2^2}{C_0} \right]}{\left[ 1 + \frac{2K_1^2 v^2 a^2 \pi^2}{L^2} \right]} . \quad (85)$$

This equation is identical to the dispersion curve relationship for the improved elastic wave in Chapter II and represents an imaginary material for which  $\alpha = 0$ . However,  $\alpha = 0$  is not a valid physical approximation as we shall see in the following discussion.

### C. Coupled Solution

For all materials considered, the coupling coefficient is very small. This fact, along with the fact that a computerized solution of the sixth order roots of equation (79) would be required, suggested the use of a perturbation technique. To condense the notation, we use a characteristic frequency  $\omega^*$  to define the nondimensional quantities as suggested by Chadwick (1962):

$$\chi = \frac{\omega}{\omega^*} \quad (86)$$

$$\xi = \frac{V\eta}{\omega^*} \quad (87)$$

$$\omega^* = \frac{\rho C \epsilon C_0^2}{k} . \quad (88)$$

Using these quantities defined in equation (79), we obtain

$$(\chi + i\xi^2)[\xi^2(1 - d^2v^2\chi^2) + c^2v^2\xi^4 - \chi^2] + \epsilon\xi^2\chi = 0, \quad (89)$$

where

$$c^2 = \frac{K^2 a^2 \mu \rho^2 C^2 C^2}{2Ek^2 \epsilon_0}, \quad (90)$$

and

$$d^2 = \frac{K^2 a^2 \rho^2 C^2 C^2}{2k^2 \epsilon_0}. \quad (91)$$

When  $\chi$  is regarded as a real constant (assigned frequency), equation (89) is of the fourth order in  $\xi$ . However, in this discussion, the particular root corresponding to the quasi-elastic wave is desired, and therefore the form of  $\xi$  chosen is

$$\xi = \xi_0 + \delta\xi, \quad (92)$$

where  $\xi_0$  represents the improved elastic wave solution when  $\epsilon = 0$ .

The solution of equation (88) under this condition is

$$\xi_0 = \frac{-(1 - d^2v^2\chi^2) + \sqrt{(1 - d^2v^2\chi^2)^2 + 4c^2v^2\chi^2}}{2c^2v^2}. \quad (93)$$

The positive sign was chosen by comparison with equations (84) and (85).

When equation (92) is substituted into equation (89) and if higher order terms are neglected, the result can be expressed as

$$\xi = \xi_0 + \frac{-2\epsilon\xi_0\chi^2(\beta^{1/2} + \epsilon) + 12\epsilon\xi_0^3\chi\beta^{1/2}}{4\chi^2(\beta^{1/2} + \epsilon)^2 + 4\xi_0^4\beta^2}, \quad (94a)$$

where

$$(1 - d^2v^2\chi^2)^2 + 4c^2v^2\chi^2 = \beta. \quad (94b)$$

Equation (94) is of the form (when compared to equation (80))

$$\xi = C_0 \left( \frac{\chi}{V} + i \frac{q}{\omega^*} \right). \quad (95)$$

Therefore, the quasi-elastic velocity  $V$  is

$$V = \frac{C_0\chi}{\xi_{\text{real}}} = \frac{4C_0\chi[\chi^2(\beta^{1/2} + \epsilon)^2 + \xi_0^4\beta^2]}{\xi_0[1 - 2\epsilon\chi^2(\beta^{1/2} + \epsilon)]}, \quad (96)$$

and the damping coefficient  $q$  is

$$q = \frac{\omega^* \xi_{\text{imag}}}{C_0} = \frac{\epsilon\omega^* \xi_0^3 \beta^{1/2}}{2C_0[\chi^2(\beta^{1/2} + \epsilon) + \xi_0^4\beta^2]}. \quad (97)$$

Equations (96) and (97) represent the main contribution of this report to wave motion in a bounded thermoelastic solid.

#### D. Numerical Results

When equations (91) and (94) are solved numerically for the ratio of the thermoelastic velocity to pure elastic velocity ( $\tau$ ) as a function of the reduced frequency  $\chi$ , the results may be plotted as shown in figure 3. The data throughout this section are typical

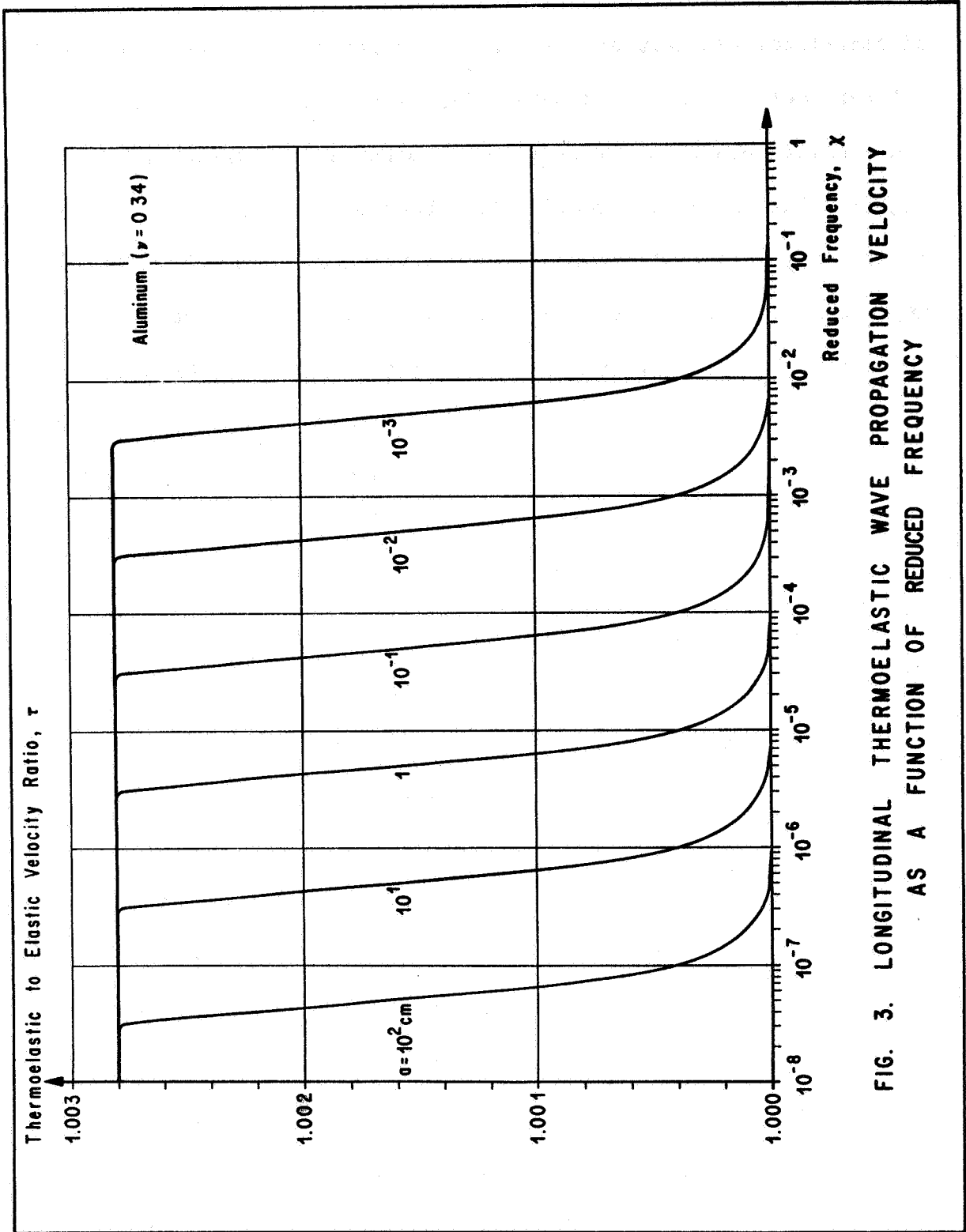


FIG. 3. LONGITUDINAL THERMOELASTIC WAVE PROPAGATION VELOCITY AS A FUNCTION OF REDUCED FREQUENCY

of structural aluminum and are shown for bar radii between  $10^{-3}$  and  $10^2$  centimeters. Figure 3 makes clear that thermal coupling modifies the elastic wave velocity by a small amount at low values of  $\chi$ . At higher values of  $\chi$ , the modification becomes negligible. The frequency at which the thermoelastic wave velocity asymptotically approaches the pure elastic velocity is a function of the bar radius. The characteristics of these curves are the same as in Chadwick. The relationship of bar radius can be eliminated from figure 3 by changing the independent variable to the ratio of bar radius to wavelength ( $a/L$ ) (see figure 4). Thus, figure 4 shows that the thermoelastic modification of elastic wave propagation velocity is primarily dependent upon the wavelength in relation to the bar radius.

Figure 5 presents the behavior of the thermoelastic damping coefficient (8) as a function of the reduced frequency ( $\chi$ ) with bar radius as a parameter. The damping coefficient ( $q$ ) varies as the square of the reduced frequency at low frequencies and asymptotically approaches a finite limiting value that is inversely dependent upon the square of the bar radius. It is clear then that very short waves traveling in small diameter rods are severely attenuated. When the same data are plotted as a function of the ratio of radius to wavelength (figure 6), the breakover point of the curves occurs when the wavelength is roughly equal to one half of the bar diameter.

The following is an example of the magnitude of this damping:  
a  $10^{-3}$  cm wave traveling in a bar of the same radius would be damped

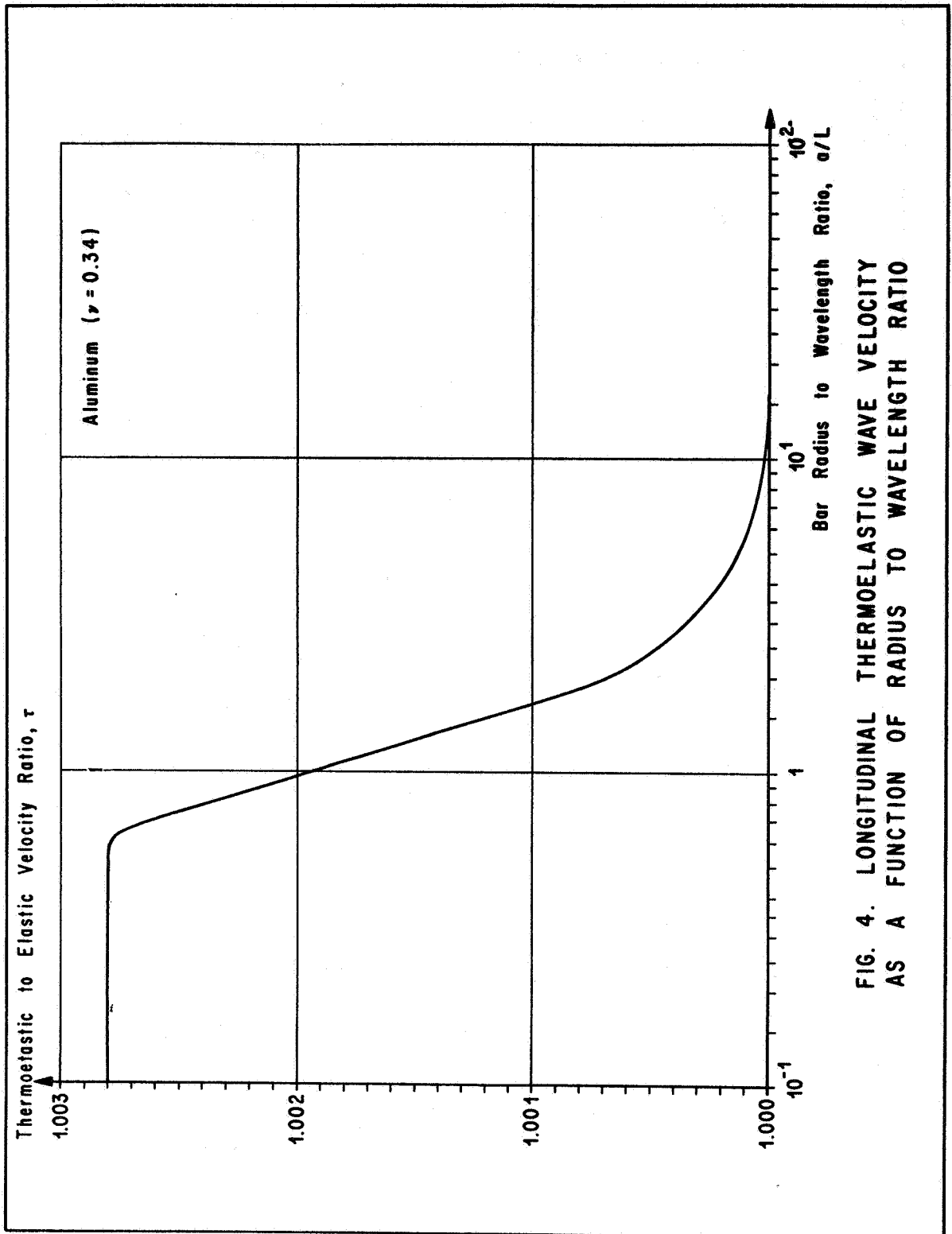


FIG. 4. LONGITUDINAL THERMOELASTIC WAVE VELOCITY AS A FUNCTION OF RADIUS TO WAVELENGTH RATIO

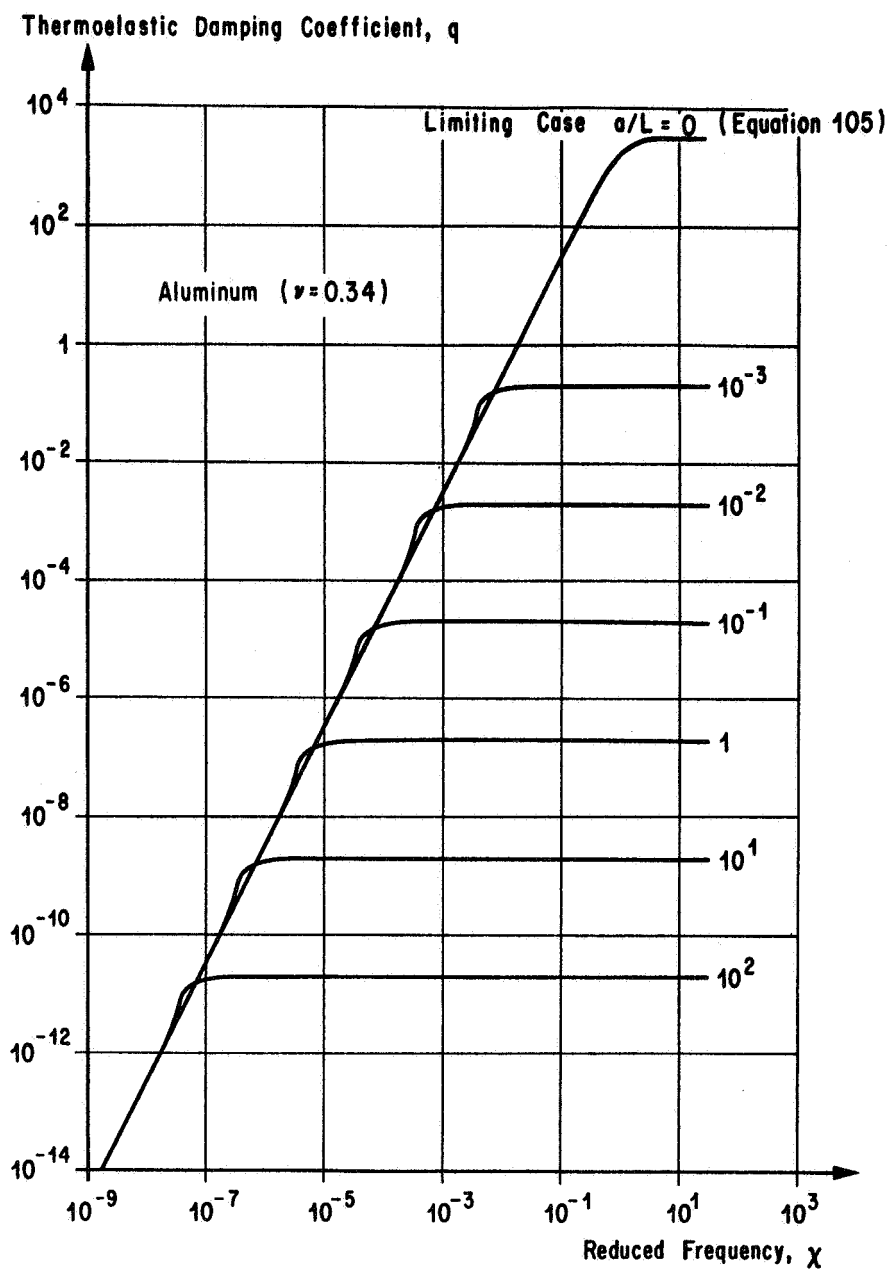


FIG. 5. THERMOELASTIC DAMPING COEFFICIENT AS A FUNCTION OF REDUCED FREQUENCY

Thermoelastic Damping Coefficient,  $q$

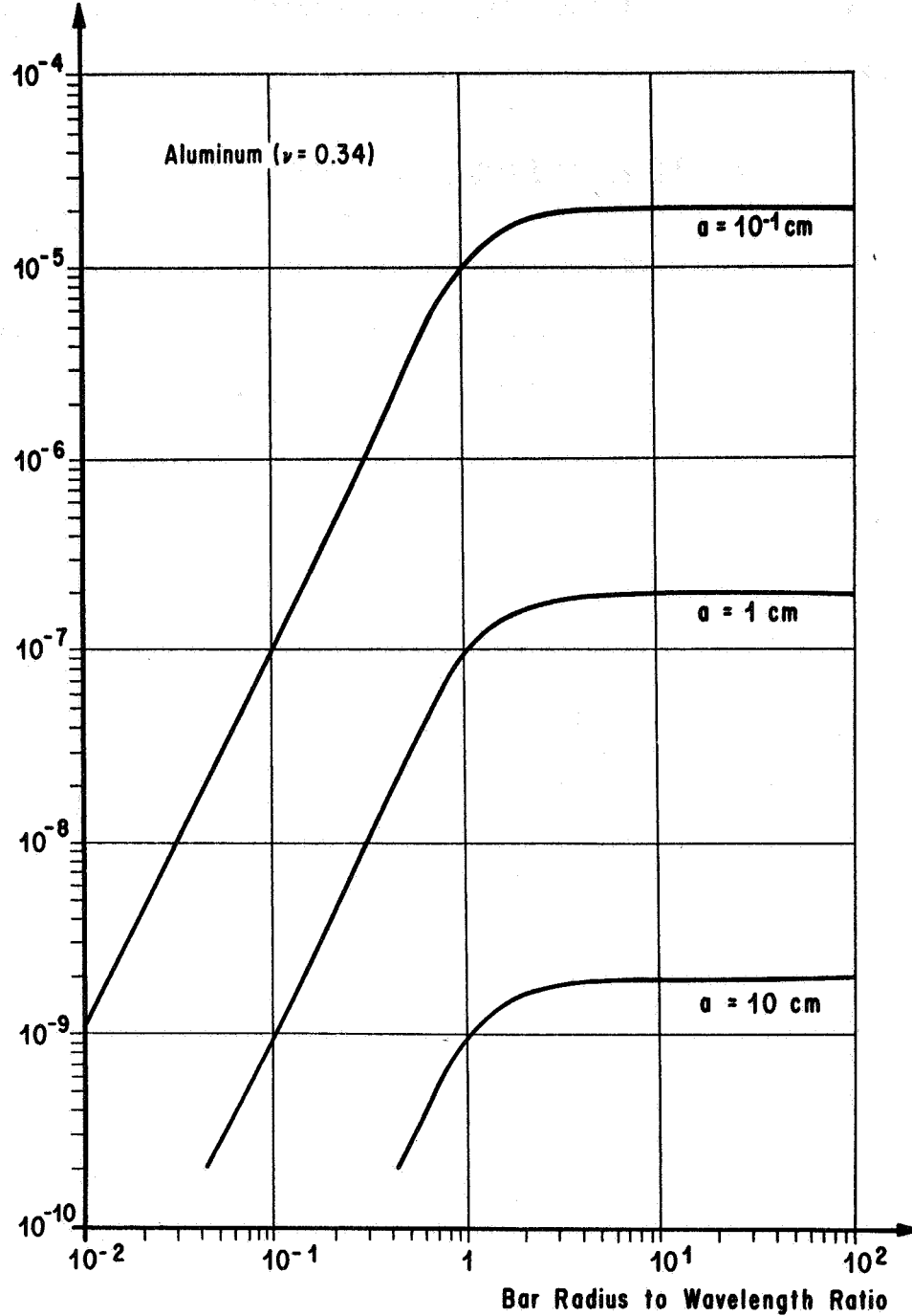


FIG. 6. THERMOELASTIC DAMPING COEFFICIENT AS A FUNCTION OF RADIUS TO WAVELENGTH RATIO

to half amplitude in 6.93 cm. As a more practical case, a one centimeter wave in a bar of the same radius would decay to half amplitude in 69.3 kilometers.

#### E. Limiting Case for a/L Approaching Zero

The above results for thermoelastic rods can be compared with Chadwick's results for an infinite thermoelastic solid by noting the behavior of equations (93), (96), and (97) at large wavelengths. When a/L approaches zero, equations (90) and (91) approach zero and equation (89) becomes

$$(\chi + i\xi)(\xi^2 - \chi^2) + \epsilon\xi^2\chi = 0, \quad (98)$$

which is exactly Chadwick's result.

The uncoupled solution of equation (98) is

$$\xi_0^2 = \chi^2 \quad (99)$$

and

$$\xi_0^2 = i\chi. \quad (100)$$

Equation (99) corresponds to the elastic wave and equation (100) to the thermal mode. Using equation (99) and the perturbation form, equation (92), and ignoring higher orders of  $\epsilon$ , we obtain

$$\xi_{\text{real}} = \frac{\chi(1 - \epsilon)}{2[(1 + 2\epsilon) + \chi^2]} \quad (101)$$

and

$$\xi_{\text{imag}} = \frac{\epsilon\chi^2}{2[(1 + 2\epsilon) + \chi^2]} \quad (102)$$

When equation (101) is used with (95), the thermoelastic velocity can be written as

$$V = C_0 \left( 1 + \frac{\epsilon}{2(1 + \chi^2)} \right). \quad (103)$$

This form for the wave velocity can be shown to correspond with Chadwick's results of the first order in  $\epsilon$ . At large wavelengths ( $\chi \rightarrow 0$ ), equation (103) reduces to

$$V_{\chi \rightarrow 0} = C_0 \left( 1 + \frac{\epsilon}{2} \right). \quad (104)$$

This result is easily seen in figures 3 and 4 if we realize that  $\epsilon$  for aluminum is 0.0054. Likewise, equations (95) and (103) are used to solve for the damping coefficient,

$$q = \frac{\omega^*}{C_0} \left[ \frac{\epsilon \chi^2}{2(1 + \chi^2)} \right]. \quad (105)$$

Equation (105) corresponds to the results of Chadwick (to the first order in  $\epsilon$ ) and is shown in figure 5. The reason that the damping coefficients predicted by the present theory exceed the value obtained for the limiting case may be seen by taking the ratio of equation (97) to equation (105). At small wavelength ( $\chi \rightarrow \infty$ ), equation (105) reduces to

$$q_{\chi \rightarrow \infty} = \frac{\omega^* \epsilon}{2C_0}. \quad (106)$$

The elastic velocity of the present solution is  $C_0$  instead of  $C_1$  in the Chadwick solution because, in the present theory, the dilatation is expressed as

$$\Delta = (1 - 2\nu) \frac{\partial W}{\partial z} \quad (107)$$

instead of the form of equation (3). The thermoelastic behavior for small values of radius to wavelength ratio is the same, with the exception of dilatational velocity, as reported in Chadwick's analysis of an infinite thermoelastic solid.

#### F. Thermoelastic Bar Number

The general behavior of the damping coefficient can be more clearly seen if we observe that, in practice,  $\chi$  will be very much smaller than one, since  $\omega^*$  is in the order of  $10^{11}$  radians per second. Using this fact, we can approximate the behavior of  $q$  as a function of  $\chi$ . Consider the behavior of equations (93) and (94) when  $d\nu\chi$  (thus, also  $c\nu\chi$ ) is less than one. Equation (93) yields

$$\xi_0 = \chi, \quad (108)$$

and equation (97) yields

$$q = \frac{\omega^* \epsilon \chi^2}{2C_0}. \quad (109)$$

Equation (105) neatly expresses the behavior of the damping coefficient as a function of  $\chi^2$ . When  $d\nu\chi$  is greater than one, equation (93) yields

$$\xi_0 = \frac{d}{c} \chi, \quad (110)$$

and equation (97) yields

$$q = \frac{\omega^* \epsilon d}{2C_0 c^3 \nu^2}. \quad (111)$$

Equation (107) then predicts the value of  $q$  at very high frequencies. At the particular value of  $\chi$  for which  $d\nu\chi$  is identically one, equation (93) reduces to

$$\xi_0 = \frac{\chi}{c\nu}. \quad (112)$$

The damping coefficient, equation (97), is thus

$$q = \frac{\omega^* \epsilon}{4C_0 c^2 \nu^2} \frac{c}{d}. \quad (113)$$

This point corresponds to a maximum slope condition and can be used as a demarcation point for the approximations contained in equations (109) and (111). Thus, the behavior of the damping coefficient can be approximated by equations (109), (111), and (113). A specific example is shown in figure 7 for an aluminum bar of 1 centimeter radius. Thus, the parameter  $d\nu\chi$  has been shown to be of primary importance to the behavior of the thermoelastic damping coefficient in a cylindrical rod.

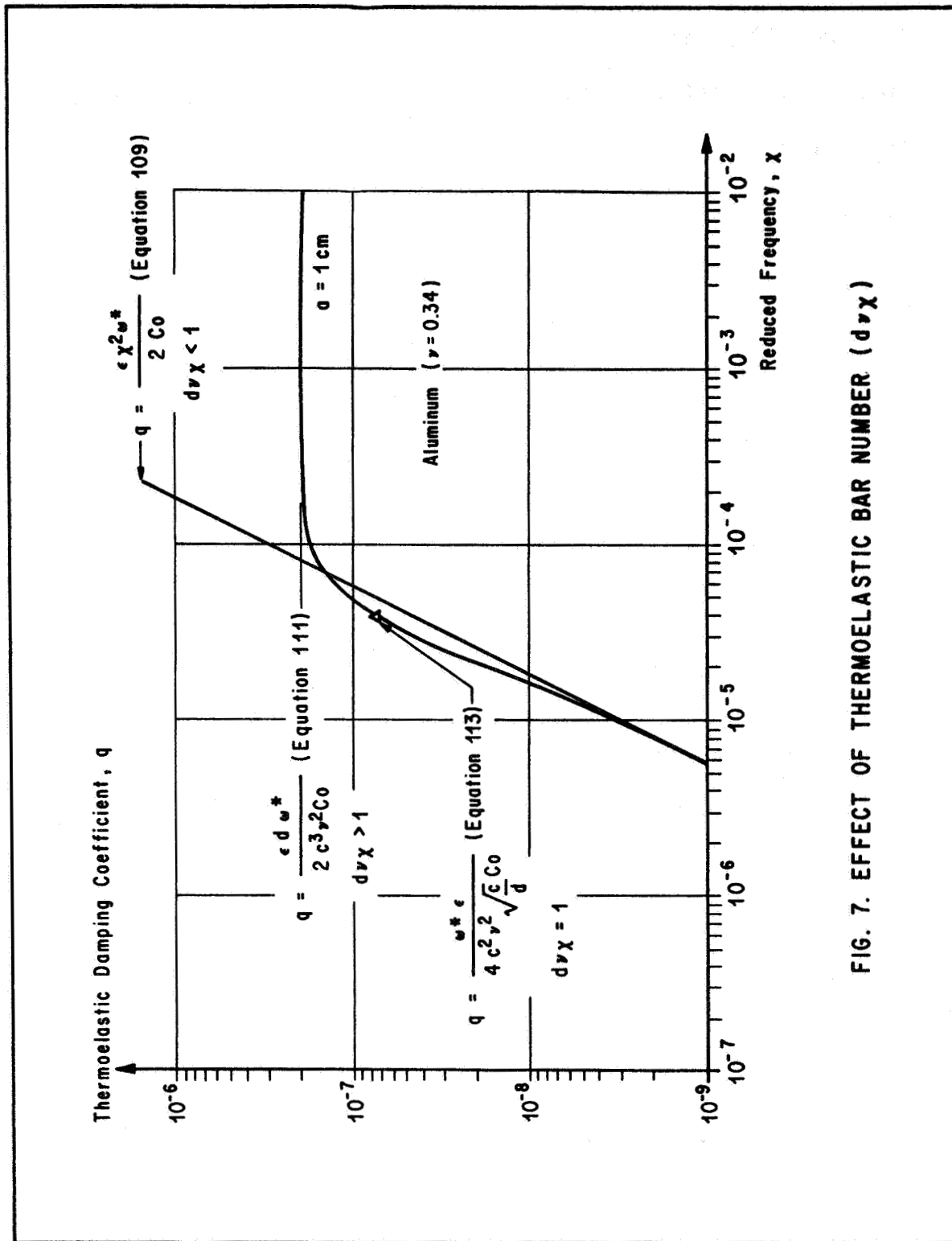


FIG. 7. EFFECT OF THERMOELASTIC BAR NUMBER ( $d\nu\chi$ )

## CONCLUSIONS

This study considers longitudinal thermoelastic wave propagation in cylindrical rods. More specifically, the thermoelastic effects on an assigned frequency wave are shown to be small in terms of the propagation velocity. However, in comparison, the thermoelastic damping effect is large for very high frequency waves traveling in small diameter bars. The behavior of the thermoelastic damping coefficient is linked to the "thermoelastic bar number"  $d\sqrt{\chi}$ , developed herein. Finally, approximations are developed, based upon the value of the thermoelastic bar number, to predict the behavior of the thermoelastic damping coefficient as a function of frequency.

It is hoped that this report provides a basis upon which investigations into thermoelastic effects on other structural elements will proceed.

## BIBLIOGRAPHY

### Books

- Kolsky, H., Stress Waves in Solids, 1963, Dover, New York.
- Love, A. E. H., A Treatise on the Mathematical Theory of Elasticity, 1944, Dover, New York.
- Nowacki, W., Thermoelasticity, 1962, Addison Wesley, Reading, Mass.
- Rayleigh, J. W. S., The Theory of Sound, Volume 1, 1945, Dover, New York.
- Sneddon, I. N. and R. Hill, Progress in Solid Mechanics, 1960, North-Holland, Amsterdam.

### Articles

- Bishop, R. E. D., *The Aeronautical Quarterly*, Volume III, February 1952, page 280.
- Chadwick, P., *Journal of the Mechanics and Physics of Solids*, Volume 10, 1962, page 99.
- Mindlin, R. D. and G. Herrmann, *Applied Mechanics Review*, Number 5, 1951, page 1308.
- Zaker, T. A., *Stress Waves Generated by Heat Addition in an Elastic Solid*, American Society of Mechanical Engineers, Paper 64-WA/APM-22, 1964.

## DAMPING OF THERMOELASTIC STRUCTURES

by William Mitchell Gillis

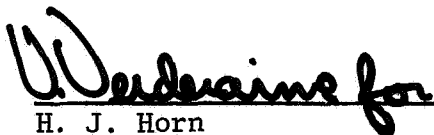
The information in this report has been reviewed for security classification. Review of any information concerning Department of Defense or Atomic Energy Commission programs has been made by the MSFC Security Classification Officer. This report, in its entirety, has been determined to be unclassified.

This document has also been reviewed and approved for technical accuracy.



---

E. I. Deaton  
Chief, Mission Analysis Branch



---

H. J. Horn  
Chief, Dynamics and Flight Mechanics Division



---

E. D. Geissler  
Director, Aero-Astroynamics Laboratory

DISTRIBUTION

DIR

Northrop Space Laboratories  
Huntsville, Ala. 35805  
Attn: Dr. S. Hu

DEP-T

R-P&VE

Mr. Kroll  
Mr. Farrow  
Dr. Lucas

Univ. of Ala. Res. Inst.  
Huntsville, Ala. 35805  
Attn: Dr. E. V. Wilms  
Dr. J. J. Brainerd  
Dr. J. T. Oden  
Dr. F. C. Liu

R-AS-DIR

Mr. Williams

R-ASTR

Dr. Haeussermann

R-COMP

Dr. Hoelzer

R-SSL-DIR

Dr. Stuhlinger

R-AERO

Dr. Geissler  
Mr. Jean  
Mr. Horn  
Mr. Verderaime  
Mr. T. Deaton  
Mr. Rheinfurth  
Mr. Ryan  
Mr. Perrine  
Dr. F. Krause  
Mr. Chandler  
Mr. Baker  
Mr. Gillis (10)

MS-IP

MS-IL (8)

CC-P

I-RM-M

MS-H

MS-T (6)

Scientific and Technical Info. Facility (25)

Box 33

College Park, Md.

Attn: NASA Rep. (S-AK/RKT)